Journal of the Chinese Advanced Materials Society

Oxide ionic conductivity properties of binary δ-(Bi₂O₃)₁ ₋ ₓ (Yb₂O₃) ₓ system

Nilgun Ozpozan Kalaycioglu [a], Esra Öztürk [b] & Serkan Dayan [a]

[a] Department of Chemistry, Faculty of Science, Erciyes University, Kayseri, Turkey

[b] Department of Materials Science and Engineering, Faculty of Engineering, Karamanoğlu Mehmetbey University, Karaman, Turkey

PLEASE SCROLL DOWN FOR ARTICLE

Taylor & Francis
Taylor & Francis Group

Oxide ionic conductivity properties of binary δ-(Bi$_2$O$_3$)$_{1-x}$(Yb$_2$O$_3$)$_x$ system

Nilgun Ozpozan Kalaycioglu[a], Esra Öztürk[b*] and Serkan Dayan[a]

[a]Department of Chemistry, Faculty of Science, Erciyes University, Kayseri, Turkey;
[b]Department of Materials Science and Engineering, Faculty of Engineering, Karamanoğlu Mehmetbey University, Karaman, Turkey

In this study, after doping ytterbium oxide (Yb$_2$O$_3$) to α-bismuth trioxide (α-Bi$_2$O$_3$) in the range of $9\% \leq n \leq 20\%$ in a series of different mole ratios, heat treatment was performed by applying a cascade temperature rise in the range of 700–790°C for 48 hours and new phases were obtained in the (Bi$_2$O$_3$)$_{1-x}$(Yb$_2$O$_3$)$_x$ system. After 24 hours of heat treatment at 700°C and 750°C and 48 hours of heat treatment at 790°C, mixtures containing 9–20 mol% Yb$_2$O$_3$ formed a face-centered cubic phase. With the help of X-ray diffraction (XRD), the crystal systems and lattice parameters of the solid solutions were obtained and their characterization was carried out. The surfaces of the solid solutions were detected by a scanning electron microscope (SEM). Thermal measurements were made by using a simultaneous DTA/TGA (differential thermal analysis/thermogravimetric analysis) system. The total conductivity (σT) in the δ-Bi$_2$O$_3$ doped with Yb$_2$O$_3$ system was measured using the four-probe DC method.

Keywords: oxides; ionic conductivity; X-ray diffraction; electron microscopy

1. Introduction

Until now, researchers have reported six polymorphs of bismuth trioxide (Bi$_2$O$_3$). These are the monoclinic (α-Bi$_2$O$_3$), body-centered cubic (bcc) (γ-Bi$_2$O$_3$), face-centered cubic (fcc) (δ-Bi$_2$O$_3$), tetragonal (β-Bi$_2$O$_3$), triclinic (ω-Bi$_2$O$_3$), and orthorhombic (ε-Bi$_2$O$_3$) phases [1–7]. The α-phase is stable at room temperature, while the other five forms are unstable crystal modifications that are formed at high temperatures. If pure α-Bi$_2$O$_3$, whose melting temperature is 824°C, is heated until around 729°C, it transforms into the δ-Bi$_2$O$_3$ phase, which is stable at high temperature and up to the melting point. When it is cooled again, it transforms into the β-Bi$_2$O$_3$ phase at ∼650°C and the γ-Bi$_2$O$_3$ phase at ∼639°C. If the β- and γ-phases are cooled to lower temperatures, they transform into the α-Bi$_2$O$_3$ phase again at around ∼500°C. Orthorhombic (ε-Bi$_2$O$_3$) and triclinic phases (ω-Bi$_2$O$_3$), on which there is scarce information, can be obtained with notable special synthesis reactions and hydrothermal heat treatment processes at 240°C and 800°C, respectively [3,8].

Bismuth oxide systems exhibit high oxide ion conductivity and have been proposed as good electrolyte materials for applications such as solid oxide fuel cells and oxygen sensors. However, due to their instability under conditions of low oxygen partial pressures, there has been difficulty in developing these materials as alternative electrolyte materials compared with the state-of-the-art cubic stabilized zirconia electrolyte. Bi$_2$O$_3$ polymorphs have important scientific and industrial uses. For example, they are used in the construc-

tion of ceramic solid fuel cell electrodes and membranes, in the catalysis of some heterogeneous reactions, in the partial oxidation of hydrocarbons, and in the removal of the harmful effects of exhaust gases as catalytic converters. The other most important area of use is the production of electrochemical energy [1,9–19].

2. Experimental

Ytterbium oxide (Yb_2O_3) was added to α-Bi_2O_3 in the range of 9% $\leq n \leq$ 20% mol in different ratios. The combined substances were grinded in an agate mortar to achieve a solid-state reaction and were subjected to 24 and 48 hours of heat treatment in a porcelain crucible. The mixtures were heat-treated at 700°C, 750°C, and 790°C. After each reaction, the products were cooled gradually until they reached room temperature.

After each solid-state reaction, the product was examined to detect whether there was a change in each powder sample's mass. Powder patterns were recorded using the X-ray diffraction (XRD) method and their crystal systems were detected. XRD data were recorded with a Bruker AXS D8 Advance model diffractometer (Bragg–Brentano geometry, graphite monochromator with CuK$_\alpha$ radiation, 0.002° pitch angle, 2Θ = 10°–90°).

The analysis of microstructure properties of the powder samples' surfaces and the microprobe analysis were performed at three different locations of solid solutions using a LEO 440 model scanning electron microscope (SEM).

Thermal measurements were made by using a simultaneous DTA/TGA (differential thermal analysis/thermogravimetric analysis) system (Shimadzu FC-60 type). The samples of δ-Bi_2O_3 doped with Yb_2O_3 were heated at a rate of 10°C min^{-1} from room temperature to 830°C. Measurements were made in a 60 mL min^{-1} nitrogen atmosphere using a platinum sample holder and an α-Al_2O_3 inert reference substance.

The total electrical conductivity (σ_T) measurements were made on samples pelletized (diameter 10 mm, thickness ~1 mm) using a four-probe DC method in the temperature range 100°C–750°C. To reduce contact resistance, fine platinum wires were attached directly to the surface of the samples. All data were recorded by a Keithley 2400 source meter and a Keithley 2700 electrometer, which were controlled by a computer.

3. Results and discussion

The minimum temperature needed to obtain a crystal system that is stable in its single phase under reaction circumstances is 750°C. Solid solutions were obtained in δ-Bi_2O_3 crystallized in a face-centered cubic crystal system in the $(Bi_2O_3)_{1-x}(Yb_2O_3)_x$ system in the range of 0.09 $\leq x \leq$ 0.20 mol fractions. The powder patterns of 15 mol% Yb_2O_3 doped the solid solutions are given in Figure 1 as a sample.

All the designs of the samples indexed in the face-centered cubic crystal system show a similarity with the designs in Figure 1. The change in unit cell parameters in these powder samples with the amount of Yb_2O_3 doped is presented in Figure 2. Fifteen mol% Yb_2O_3-doped solid solutions' SEM images are given in Figure 3. The microstructures of the substances consisted of regular fine grains with an average size of about 0.5–2.5 μm.

In Figure 4, the electrical conductivity plots of δ-Bi_2O_3 doped with 12 mol% Yb_2O_3, 14 mol% Yb_2O_3, 15 mol% Yb_2O_3, and 16 mol% Yb_2O_3 contents are presented, and the σ_T plots for the other δ-Bi_2O_3 phases are quite similar. These data were obtained during a repeated heating run at a constant heating rate in air. The electrical conductivity of δ-Bi_2O_3 doped with 9–20 mol% Yb_2O_3 increased with increasing temperature up to ~634°C. Beyond this temperature, the conductivity increased sharply up to about 670°C.

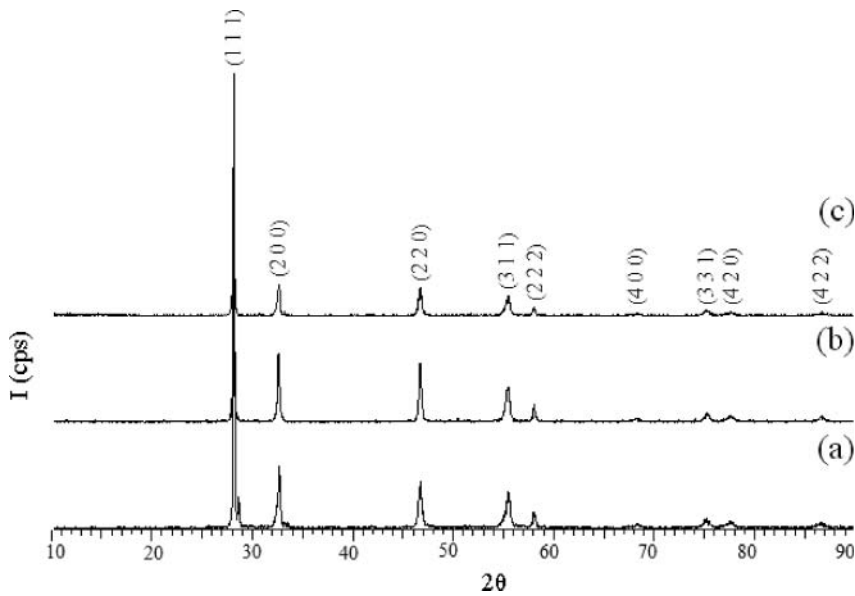Figure 1.   XRD patterns of δ-Bi$_2$O$_3$ doped with 15% mol Yb$_2$O$_3$ (a) at 700°C, (b) at 750°C, and (c) at 790°C.

The reason for the sharp increase in the conductivity was the phase formation and an alteration in the crystal structure, possibly causing a change in the conductivity mechanism. Structural disorder during the phase formation may also contribute to the improvement in ionic conductivity. Actually, the DTA/TGA measurements also suggested that a polymorphic formation took place, and the endothermic phase transition was observed on the DTA curve at about the same temperature range (Figure 5). As can be seen from Figure 4, the formation temperature is $\sim$637°C, which was determined by DTA; the transition temperature in the conductivity versus temperature graph is in the range of 634–670°C. The mass of substance was not changed in the 50–1000°C temperature range in the TGA ther-
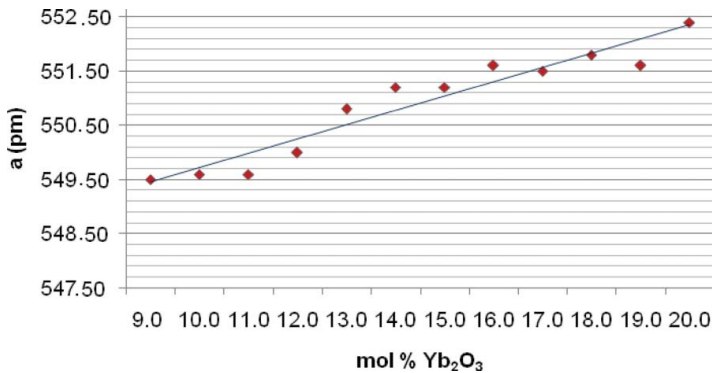

Figure 2.   The relationship between the amount of Yb$_2$O$_3$ doping and the lattice parameter of δ-Bi$_2$O$_3$.
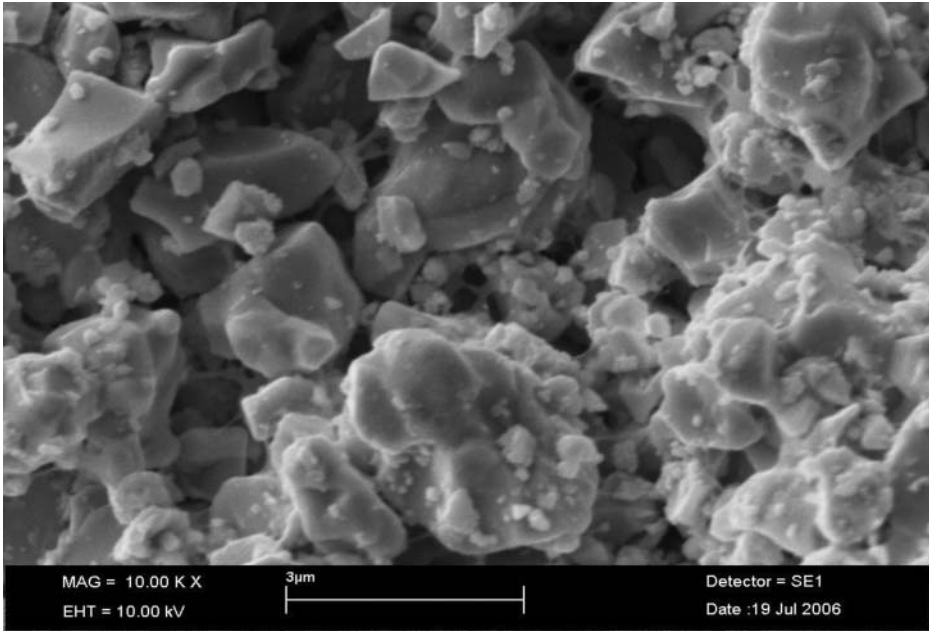
Figure 3. SEM image of δ-Bi$_2$O$_3$ doped with 15% mol Yb$_2$O$_3$.
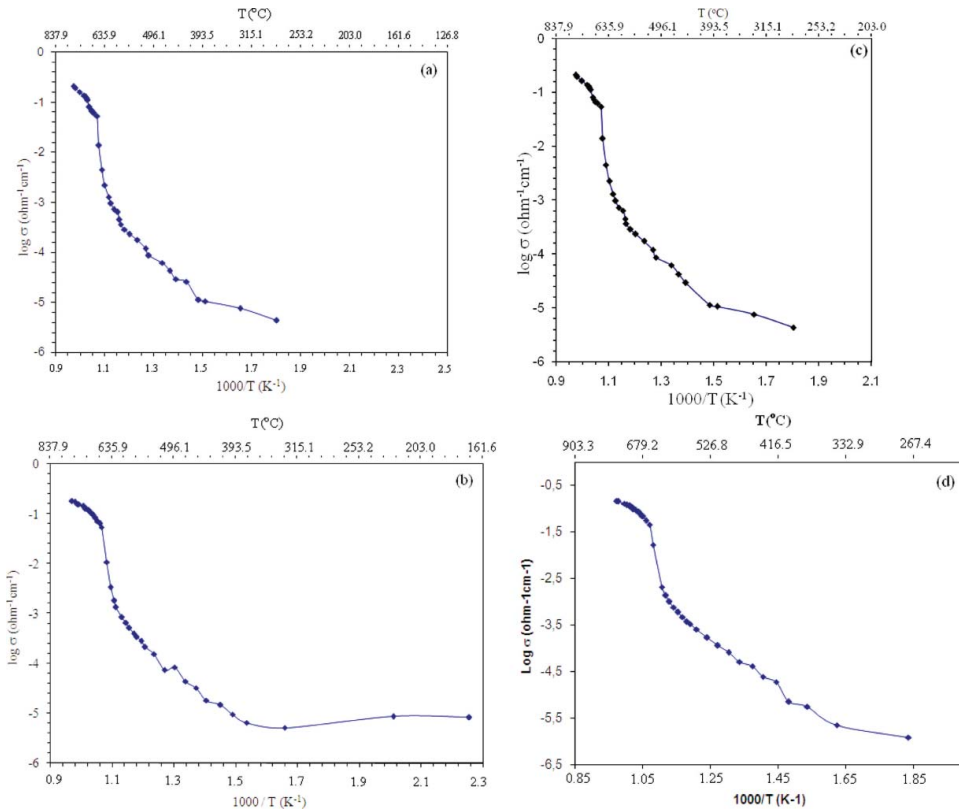
Figure 4. Arrhenius plots of electrical conductivity for δ-Bi$_2$O$_3$ doped with (a) 12 mol% Yb$_2$O$_3$, (b) 14 mol% Yb$_2$O$_3$, (c) 15 mol% Yb$_2$O$_3$, and (d) 16 mol% Yb$_2$O$_3$.
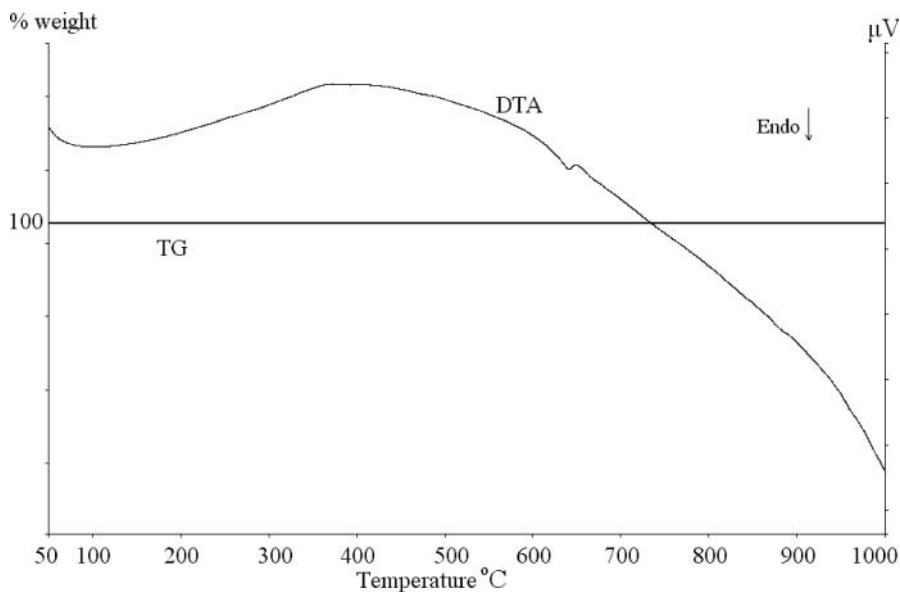
Figure 5.   DTA/TG diagrams of δ-Bi_2O_3 phase doped with 15 mol% Yb_2O_3.

mogram, and the DTA curve shows the endothermic peak in the range of 620–651°C, which shows δ-Bi_2O_3 phase formation.

Producing a phase in the $(Bi_2O_3)_{1-x}(Yb_2O_3)_x$ system requires a long duration of heat application. In solid-state reactions that take place at high temperature, ytterbium (III) ions are diffused gradually into the Bi_2O_3 lattice. If the doping process is successful, diffused ytterbium (III) cations prefer to change place with bismuth (III) cations in the lattice. This situation is thought to cause nonstoichiometry and transformation to a defect structure in the lattice as well as to cause O^{2-} ion conductivity.

The experimental results showed that in our samples, the oxygen lattice points of the δ-Bi_2O_3 doped with ytterbium (III) were not completely occupied with oxygen ions. If the oxygen sublattices were fully occupied by O^{2-} ions, the Yb_2O_3-doped δ-Bi_2O_3 phases would not show such a high degree of electrical conductivity. Some of the oxygen lattice points located around the tetrahedral sites may have been vacant, forming an oxygen vacancy. These oxygen vacancies were filled randomly with neighboring oxygen ions at an increasing rate with increasing temperature. Jumping oxygen ions left their former sites vacant; thus, another vacancy was formed. Since this process was random, the total oxygen flow was zero in any direction without an applied electric field [20].

The conductivity of δ-Bi_2O_3 phases doped with Yb_2O_3 increased with increasing temperature. It was proposed that this was related to ionic mobility, which rises with increasing temperature. At elevated temperatures, the thermal vibrational energy of the ions increased, causing a higher oxygen ion-jumping rate. Although oxygen vacancies were present in the crystal structure at low temperatures (below 150°C), the thermal energy of the anions was not high enough for them to jump out of their lowest energy positions. Thermal vibrations may also have assisted in the jumping process for a short time by either shortening the jumping distance or by widening the jumping channels through the crystal [21].

4. Conclusions

As a result of this research, the δ-phases of Bi_2O_3 that are unstable at room temperature were obtained by doping Yb_2O_3 to α-Bi_2O_3 under solid-state reactions. The effective factor in the synthesis of these polymorphs is high temperature application. In addition to this, the amount of doped Yb_2O_3 is not an effective factor at increasing or decreasing the oxygen ionic conductivity.

It can be concluded from the exchange of Yb^{3+} with crystal structured Bi^{3+} cations that nonstoichiometric phases are synthesized. Since the synthesis process was performed using a high temperature application that lasted for a long period, we can say that ytterbium cations diffuse in the crystal structure slowly. δ-phase $(Bi_2O_3)_{1-x}(Yb_2O_3)_x$ ($x = 0.09$–0.20) binary oxide compounds possessing oxygen ionic conductivity were synthesized. The nonstoichiometry of the δ-Bi_2O_3 phase was thought to lead to interesting electrical properties.

The ionic conductivity in the δ-Bi_2O_3 phase supports the view that there is an average occupation of oxide ions in oxygen lattice sites, which can move from site to site through the bismuth sublattice. The sample conductivity of -0.678 ohm^{-1} cm^{-1} at $750°C$ was the δ-phase of the $(Bi_2O_3)_{0.88}(Yb_2O_3)_{0.12}$ system. The other samples conductivities were observed between -0.737 and -0.837 ohm^{-1} cm^{-1} at $750°C$. When these results are compared with the results of our other studies [20,21], it seems that the conductivities of δ-$(Bi_2O_3)_{1-x}(Yb_2O_3)_x$ system are lower than the conductivities of δ-$(Bi_2O_3)_{1-x}(Tb_4O_7)_x$, β-$(Bi_2O_3)_{1-x}(Tb_4O_7)_x$, and δ-$(Bi_2O_3)_{1-x}(Lu_2O_3)_x$ systems.

References

[1] Sammes NM, Tompsett GA, Nafe H, Aldinger F. Bismuth based oxide electrolytes — Structure and ionic conductivity. J Eur Ceram Soc. 1999;19:1801–1826.
[2] Leontie L, Caraman M, Delibaş M, Rusu GI. Optical properties of bismuth trioxide thin films. Mater Res Bull. 2001;36:1629–1637.
[3] Harwig HA. On the structure of bismuthsesquioxide: The α, β, γ and δ phase. Anorg Allg Chem. 1978;444:151–166.
[4] Chehab S, Conflant P, Drache M, Boivin J-C, McDonald G. Solid-state reaction pathways of sillenite-phase formation studied by high-temperature X-ray diffractometry and differential thermal analysis. Mater Res Bull. 2003;38:875–897.
[5] Takahashi T, Esaka T, Iwahara H. Oxide ion conduction in the sintered oxides of MoO_3-doped Bi_2O_3. J Appl Electrochem. 1977;7:31–35.
[6] Crumpton TE, Francesconi ME, Greaves C. The structural chemistry of $Bi_{14}MO_{24}$ (M = Cr, Mo, W) phases: Bismuth oxides containing discrete MO_4 tetrahedra. J Solid State Chem. 2003;175:197–206.
[7] Ekhelikar S, Bichile GK. Synthesis and structural characterization of $(Bi_2O_3)_{(1-x)}$ $(Y_2O_3)_{(x)}$ and $(Bi_2O_3)_{(1-x)}$ $(Gd_2O_3)_x$ solid solutions. Bull Mater Sci. 2004;27:19–22.
[8] Drache M, Roussel P, Wignacourt J-P. Structures and oxide mobility in Bi-Ln-O materials: Heritage of Bi_2O_3. Chem Rev. 2007;107:80–96.
[9] Arora N, Deo G, Wachs IE, Hirt AM. Surfaces aspects of bismuth-metal oxide catalysts. J Catalysis. 1996;1:159.
[10] Libye D, Poulsen FW, Mogensen M. Conductivity of A- and B-site doped $LaAlO_3$, $LaGaO_3$, $LaScO_3$ and $LaInO_3$ perovskites. Solid State Ionics. 2000;128:91–103.
[11] Harwig HA, Gerards AG. The polymorphism of bismuth sesquioxide. Thermochim. Acta. 1979;28:121.

[12] Goff JP, Hayes W, Hull S, Hutchings MT, Clausen KN. Defect structure of yttria-stabilized zirconia and its influence on the ionic conductivity at elevated temperatures. Phys Rev B. 1999;59:14202.

[13] Lopez-Martinez J, Romero-Serrano A, Hernandez-Ramirez A, Zeifert B, Gomez-Yanez C, Martinez-Sánchez R. Thermal analysis and prediction of phase equilibria in the TiO_2–Bi_2O_3 system. Thermochim Acta. 2011;1–2:35–39.

[14] Dutta A, Ghosh A. Ionic conductivity of Li_2O–BaO–Bi_2O_3 glasses. J Non-Crystal Solids. 2005;3:203–208.

[15] Aidhy Dipuneet S, Sinnott Susan B, Wachsman Eric D, Phillpot SR, Nino JC. Structure of δ-Bi_2O_3 from density functional theory: A systematic crystallographic analysis. J Solid State Chem. 2009;5:1222–1228.

[16] Fruth V, Dobrescu G, Bratan V, Hornoiu C, Preda S, Andronescu C, Popa M. Structural and electrochemical features of Bi_2O_3-based fast oxide ion conductors. J Eur Ceram Soc. 2007;27:4421–4424.

[17] Laurent K, Wang GY, Tusseau-Nenez S, Leprince-Wang Y. Structure and conductivity studies of electrodeposited δ-Bi_2O_3. Solid State Ionics. 2008;33–34:1735–1739.

[18] Boyapati S, Wachsman ED, Jiang NX. Effect of oxygen sublattice ordering on interstitial transport mechanism and conductivity activation energies in phase-stabilized cubic bismuth oxides. Solid State Ionics. 2001;1–2:149–160.

[19] Yaremchenko AA, Kharton VV, Naumovich EN, Tonoyan AA. Stability of δ-Bi_2O_3-based solid electrolytes. Mater Res Bull. 2000;4:515–520.

[20] Kalaycioglu NO, Çırçır E. Synthesis, characterization and oxide Ionic conductivity of binary $(Bi_2O_3)_{1-x}(Lu_2O_3)_x$ system. J Chin Chem Soc. 2011;58:1–4.

[21] Ozpozan N, Çırçır E. Measurement and properties of the oxide ionic conductivity of β- and δ-phases in the binary $(Bi_2O_3)_{1-x}(Tb_4O_7)_x$ system. Synth Reactivity Inorg, Metal-Org and Nano-Metal Chem. 2012;42:398–401.